
Mohamed Mokhles Abou-Seida, Gamal H. Elsaheed, Tarek Mohamed Salaheldin Mostafa, Elzahry Farouk Mohamed Elzahry. Experimental investigation of local three-dimensional flow field around bridge abutments in non-cohesive and cohesive soils. International Journal of Academic Research Part A; 2012; 4(4), 37-50.

EXPERIMENTAL INVESTIGATION OF LOCAL THREE-DIMENSIONAL FLOW FIELD AROUND BRIDGE ABUTMENTS IN NON-COHESIVE AND COHESIVE SOILS

Prof. Mohamed Mokhles Abou-Seida¹, Prof. Gamal H. Elsaheed²,
Lecturer, Tarek Mohamed Salaheldin Mostafa¹, Ph.D. Elzahry Farouk Mohamed Elzahry²

¹Professor, Irrigation and Hydraulics Department - Faculty of Engineering - Cairo University

²Professor, Civil Engineering Department - Faculty of Engineering, Shobra - Banha University (EGYPT)

E-mails: mokhlesas@gmail.com, gelsaheed@feng.bu.edu.eg,
tmsalaha2002@yahoo.com, elzahry@hotmail.com

ABSTRACT

The flow field around the vertical-wall abutments is investigated through detailed three-dimensional velocity measurements performed after reaching equilibrium scour bed for non cohesive soil as well as cohesive soil. Velocity measurements are taken upstream, downstream and on the side of the abutment by using the Acoustic velocity Doppler (ADV). The stagnation pressure gradient leads to downward deflection of the flow to form the downward flow at the upstream side of the abutment. The primary vortex formed at the upstream side of the abutment near the bottom rotates in downstream direction adjacent to the side of the abutment in a spiral motion. The primary vortex and secondary vortex created at the side of the abutment by flow separation extend around the abutment from side in downstream direction to form wake vortices. The flow field is used to explain the scour pattern at the vertical-wall abutments. The velocity measurements are useful for the development and validation of future flow field numerical models, which can be incorporated with scour model to estimate scour depth at bridge abutments.

Key words: Bridge abutment; cohesive soil; non-cohesive soil; experimentation; open channel flow; 3d flow field

1. INTRODUCTION

Flow in open channels or rivers are unidirectional, which becomes three-dimensional when it encounters a protruding obstacle (Graf 2002). The protrusion of a bridge abutment into the main channel or the floodplain creates a disturbance in a river flow. The flow accelerates and separates at the upstream face of the abutment as it moves past the obstacle, creating a vortex trail that moves downstream in a direction approximately perpendicular to the structure. The result is that the bed around the structure erodes locally (Lim 1997). The local scour pattern around abutments depends on the geometry of the bridge structure, local flow field as well as the type and the properties of the erodible bed (Raudkivi 1990).

The three-dimensional flow field around abutment is considered to be complex due to flow separation and generation of multiple vortices systems. The complexity of the flow field is magnified due to the dynamic interaction between the flow and the mobile bottom during the development of the scour hole. The flow field initiates and controls the progress of the scour pattern around the abutment, which in turn modifies the flow field (Raudkivi 1986). The erosion mechanism and the dominating factors upon which erosion depends are different in cohesive soil versus non-cohesive soil.

The flow structure that causes abutment local scour is complex in detail and could be separated into: Down flow, Primary vortex, Secondary vortex and Wake vortices as shown in figure (1) (Kwan 1988). Kwan was the lone investigator to detect the three-dimensional flow field in a scour hole at a vertical-wall abutment by the hydrogen bubble technique. Kwan and Melville (1994) measured the three-dimensional flow field at bridge abutments with more details by the hydrogen bubble technique. Ahmed and Rajaratnam (2000) measured the flow field at an abutment for plain (unscoured) bed condition. However, no attempt has so far been made to study the three-dimensional turbulent flow field in a scour hole at a vertical-wall abutment.

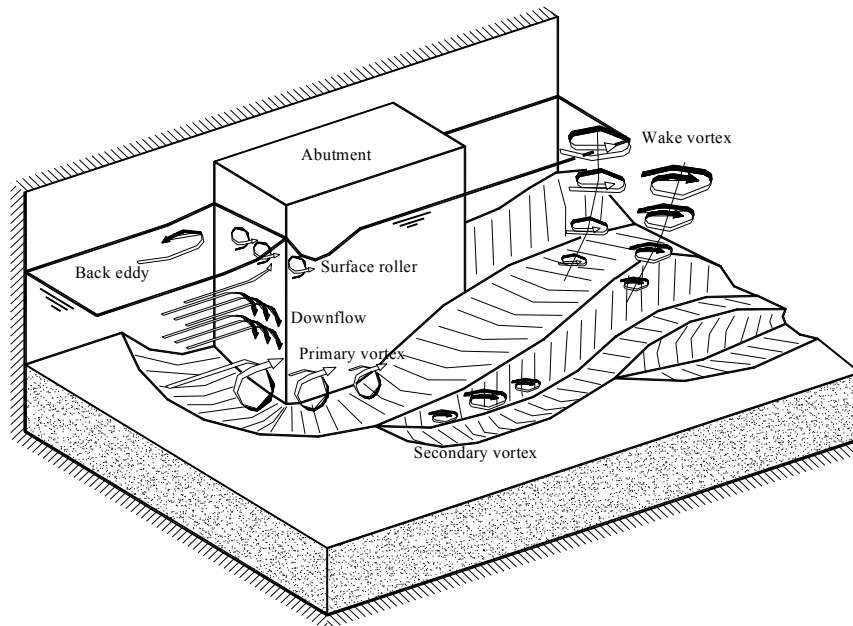


Fig. 1. Abutment flow structure (after Kwan 1988)

2. OBJECTIVE OF THE PRESENT RESEARCH

The present investigation aims to Document the flow field around bridge abutment through detailed three-dimensional velocity measurements performed with the Acoustic velocity Doppler (ADV) for non cohesive soils as well as cohesive soils. The flow field is used to explain the scour pattern at the abutments. The flow field measurements are useful for the development and validation of future flow field numerical models, which can be incorporated with scour model to estimate scour depth at bridge abutments.

3. EXPERIMENTAL PROCEDURE

The experiments are performed in a horizontal flume 7 m long, 1 m wide and 0.5 m deep. The flow goes through intake gravel tank and screen to reduce the turbulent eddies at the flume entrance. A wooden floating plate is used to absorb the surface waves. The testing section is about 1.40 m long. Three sizes of steel vertical-wall abutment are used with protrusion lengths perpendicular to the flow direction are 7.5 cm, 10 cm, and 15 cm. The abutment lengths in the flow direction are 15 cm, 20 cm, and 30 cm respectively. A calibrated Flowmeter, fitted at the inlet of the flume, is used to measure the flow discharge. The flow depth in the flume is adjusted by a tailgate. A point gauge with an accuracy of ± 0.1 mm is used to measure the flow depths.

The bed material for non cohesive soil experiments is medium sand with median size $D_{50} = 0.38$ mm and Standard Deviation = 1.7. The bed material for cohesive soil experiment is Kaolin clay. The clay content is 5%, compaction is 70%, and liquidity index is 0.25.

At the beginning of the experiment, the flume is filled with water very slowly from upstream and downstream sides. Then, the scour experiment starts with the required flow depth and flow rate. The experiments are run under a clear water scour condition for a period after which an equilibrium state of scour is achieved. The equilibrium scour condition is reached when the change of the maximum scour depth is 1 mm or less over 24 hours period of time. The maximum scour depth at the upstream nose of the abutment is measured by dipping a thin wooden rod (3 mm diameter) inside the scour hole and measuring the wetted length on that rod by a ruler with 1 mm accuracy for non cohesive soil as well as cohesive soil. Velocity measurements are taken upstream, downstream and on the side of the abutment by using the NorTek Acoustic velocity Doppler (ADV) after the equilibrium scour condition is reached.

The instantaneous three-dimensional velocity components are measured by an Acoustic Doppler Velocimeter (ADV). The acoustic sensor consists of three acoustic receivers (for 3-D probe) and one acoustic transmitter. The pulses emitted from the transmitter arrive at the measuring point (5 cm below the transmitter) and then are scattered by the water particles and the receivers receive the reflected echoes. The Doppler shifts of the reflected echoes are calculated and the three velocity components are calculated from these Doppler shifts. The data is transmitted from the Signal Conditioning Module (SCM) to the Micro-ADV-Lab processor (installed in a desktop PC that operates the data acquisition software supported by a DOS operating system) through a flexible High-Frequency Cable with an underwater mateable connector. The measurement by the down-looking ADV probe is not possible in the zone located 5 cm below the free surface (NorTek 2000). Preliminary investigation is performed in the present study to choose the appropriate sampling time and frequency. The velocity measurements taken in the present study are recorded with a sampling time of 2.0 minutes and a sampling frequency of 10 Hz.

Figure (2) shows schematic diagram of the locations of the verticals around the abutment at which velocity is measured at different points. The distances between points decreased close to the abutment to capture the details of the flow field and its alteration due to the presence of the abutment. Velocity measurements are concentrated near the flume bottom and the distance between measurements increases away from the bottom. This is done in order to capture the large velocity gradient near the bottom. The velocity measurements presented follow the sign convention in figure (3). The local velocity at any point in the directions X, Y and Z are u , v , and w respectively. The vertical axis Z represents the distance measured from the bottom. The zero value of Z represents the level of the soil surface before the scour starts and the negative Z values indicates that the measurements are taken inside the scour hole below the original bottom level.

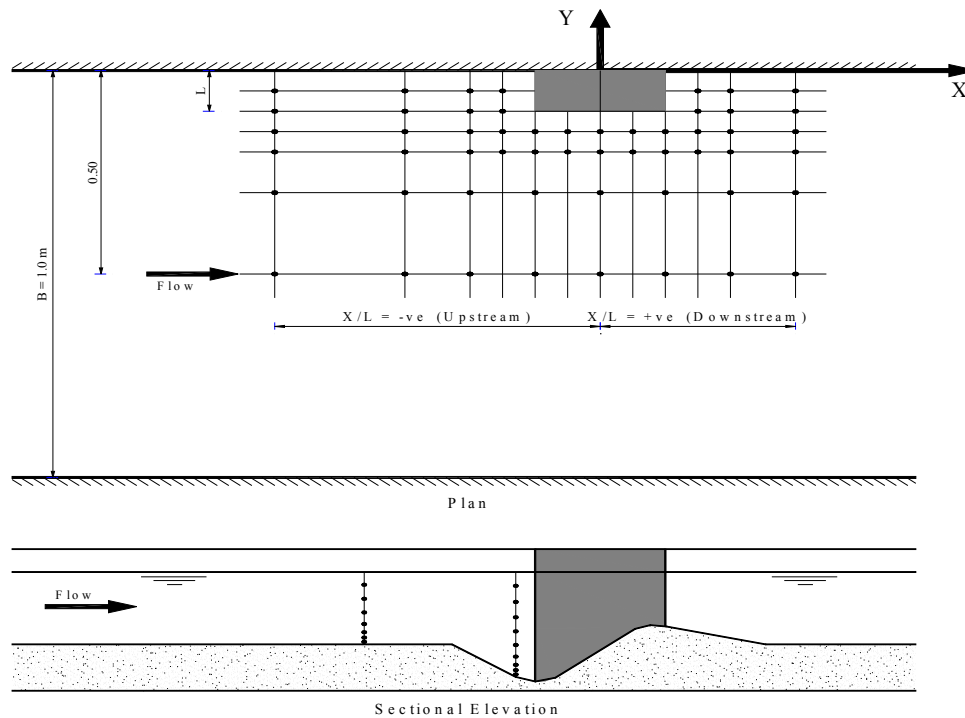


Fig. 2. Schematic diagrams showing the location of the vertical velocity profiles measured around the abutment for the scoured bottom

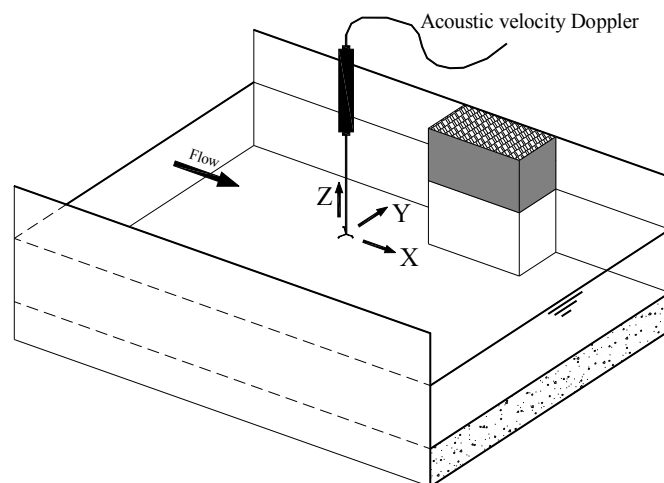


Fig. 3. Schematic diagrams showing the sign convention of the velocity measurements

4. RESULTS AND ANALYSIS

The flow field around the abutment is investigated through detailed three-dimensional velocity measurements performed in the case of equilibrium scour for non cohesive (sandy) soil as well as cohesive (clayey) soil. The dominant feature of the flow field around the abutment is captured with the velocity measurements in the present experiments. Such features included the downward flow and the primary vortex upstream of the abutment, the wake vortex and the upward flow at the downstream of the abutment, and the circulation of the primary vortex on the abutment side as shown in figure (1).

5. FLOW FIELD FOR SANDY SOIL

Table (1) gives a summary of the flow field experiments. Figures (3) to (9) show the velocity measurements for the experiment MS-7.5-5. For the details of velocity measurements for the experiments MS-10-15 and MS-15-21 (see Elzahry 2009 - Appendix A).

Table 1. Summary of the flow field experiments

Run ID	Abutment protrusion length (L) (cm)	Discharge (m ³ /s)	Flow depth (m)	Approach velocity (m/s)	Approach Froude number
MS-7.5-5	7.5	0.0292	0.120	0.243	0.207
MS-10-15	10	0.0268	0.122	0.220	0.184
MS-15-21	15	0.0229	0.121	0.189	0.159

5.1. Upstream Flow Field

Figures (4) to (6) show the vertical distribution of the streamwise velocity (u), the lateral velocity (v) and the vertical velocity (w) at different verticals in arbitrary planes (i.e. the planes passing parallel to the flow at the upstream side of the abutment).

In the planes intersecting the abutment, the flow upstream of the abutment starts to decelerate, due to the presence of the abutment, at distance 5 to 6 times abutment protrusion length (L) measured from the abutment centerline. This distance do not influenced by changing Froude number. The deceleration of the flow upstream of the abutment is noticed by a decrease in the streamwise velocity (u) as the flow approaches the abutment. Negative streamwise velocity (u) (reversed velocity) is recorded inside the scour hole Figure (4). This shows that, circulation occurred in the scour hole at the upstream side of the abutment due to the primary vortex Figure (1). The maximum value of reversed velocity (u) is 0.3 to 0.4 times the mean approach velocity.

The stagnation pressure gradient is developed in front of the abutment because the streamwise velocity (u) decreases downward from the surface. The stagnation pressure gradient leads to downward deflection of the flow to form the downward flow at the upstream side of the abutment Figure (1). The downward flow is noticed by negative velocity in the vertical direction (w) at the upstream side of the abutment Figure (6). The strength of downward flow in front of the abutment reaches a maximum just below the bed level when a scour hole is present. The maximum value of downward flow velocity (w) is 0.5 to 0.6 times the mean approach velocity. Some positive (w) velocity inside the scour hole close to the abutment shows the circulation due to the primary vortex inside the scour hole. The jet created by the downward flow pushes the bed causing it to erode sediment and then rolls up and becomes part of the primary vortex.

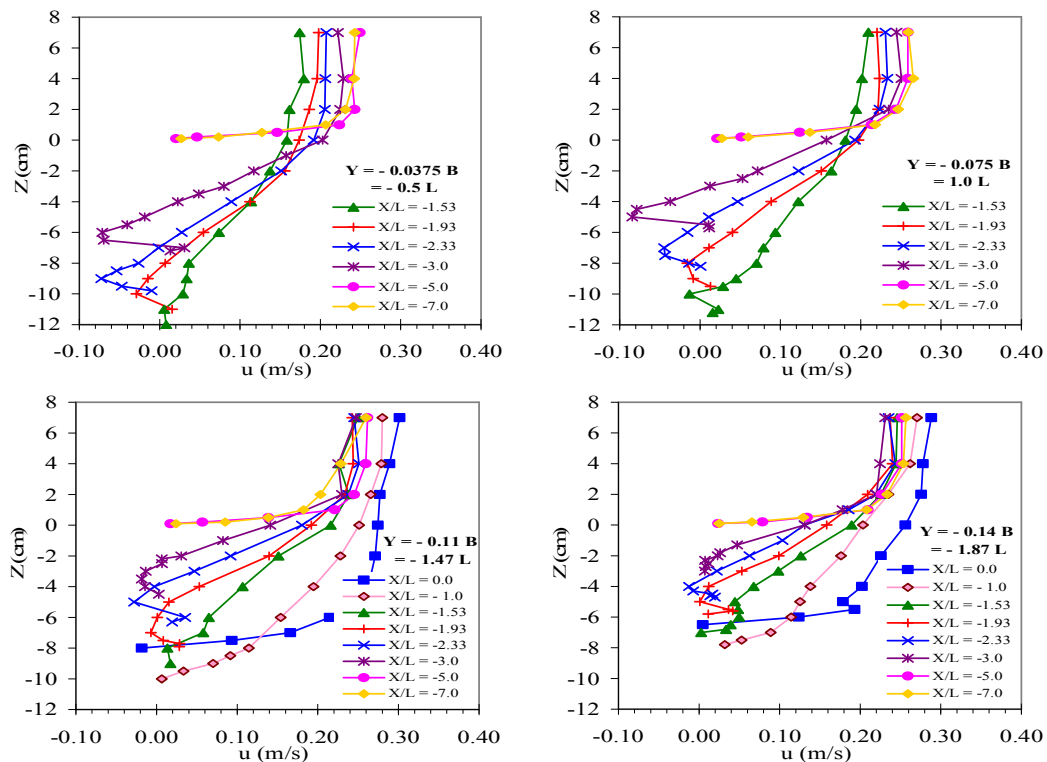


Fig. 4. Vertical profile of velocity (u) at upstream side of the abutment (MS-7.5-5)

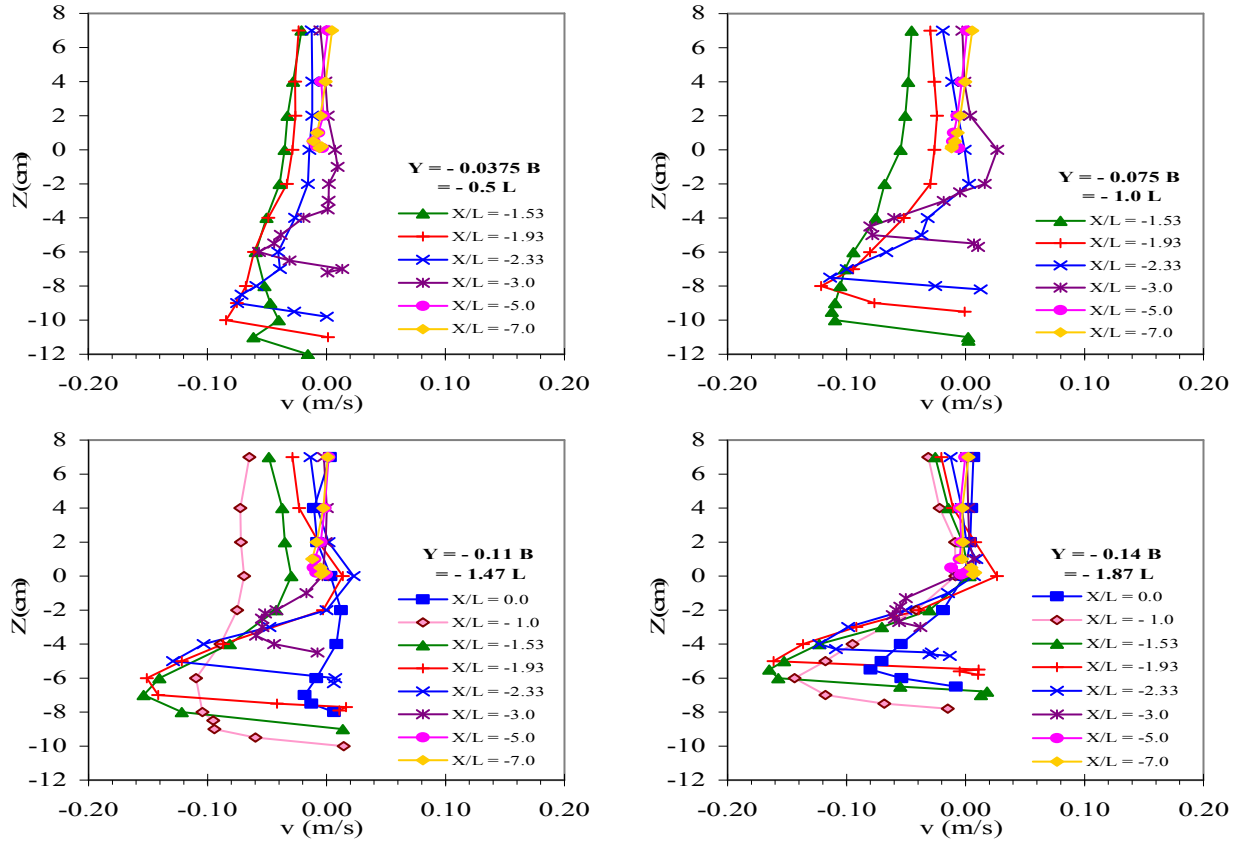


Fig. 5. Vertical profile of velocity (v) at upstream side of the abutment (MS-7.5-5)

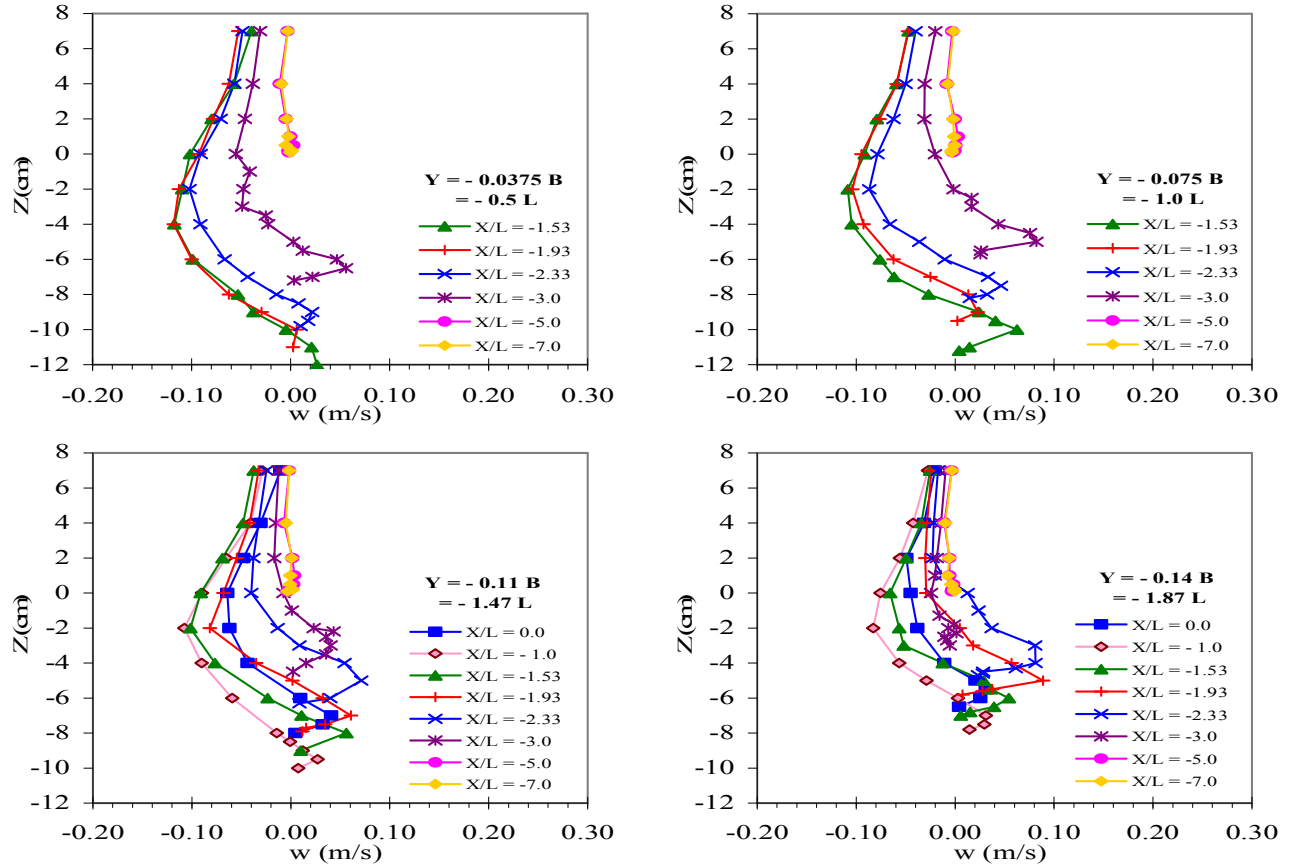


Fig. 6. Vertical profile of velocity (w) at upstream side of the abutment (MS-7.5-5)

5.2. Flow At The Side Of Abutment

Figure (7) shows the vertical distribution of the streamwise velocity (u) and the lateral velocity (v) at different verticals in planes passing perpendicular to the flow.

The primary vortex formed at the upstream side of the abutment near the bottom rotates in downstream direction adjacent to the side of the abutment in a spiral motion Figure (1).

The flow separation by the upstream abutment corner creates a surface with a discontinuity in the velocity profile and this leads to the development of secondary vortex. Secondary vortex has an opposite direction of rotation to the primary vortex Figure (1). The circulation due to the primary vortex and secondary vortex at the side of the abutment is indicated by the change of direction (sign) of the local lateral velocity (v) along the vertical distribution of (v) as shown in figure (7).

The streamwise velocity (u) increases adjacent to the side of the abutment due to the flow contraction. The maximum value of streamwise velocity (u) adjacent to the side of the abutment is 1.25 to 1.4 times the mean approach velocity.

Figure (7) shows the vertical distribution of the (u) and (v) velocities at equilibrium scour. Effect of the presence of the abutment on the streamwise velocity (u) and local lateral velocity (v) at the side of the abutment diminishes at distance 5 to 6 times abutment protrusion length (L) measured from the channel wall in lateral direction.

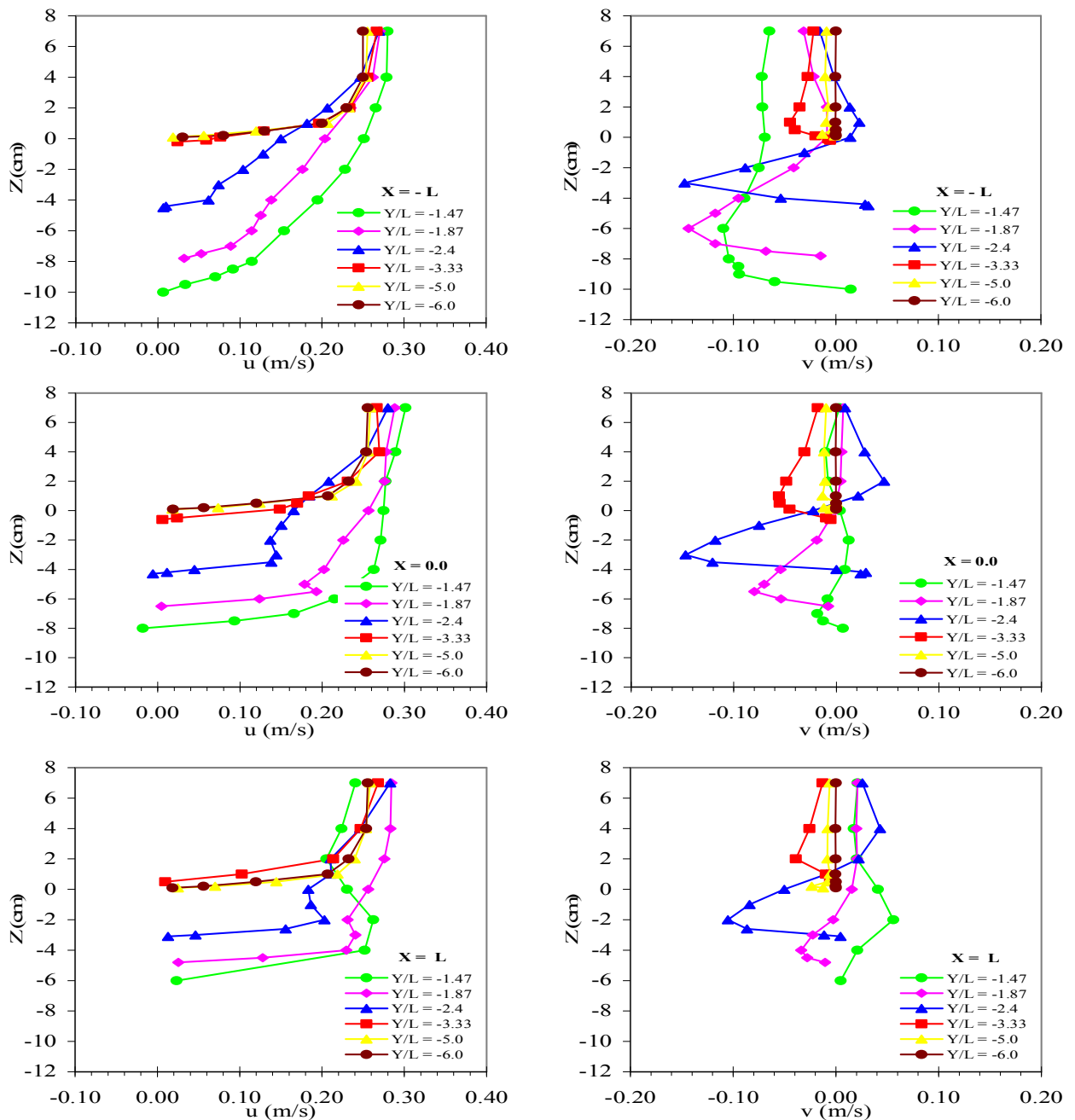


Fig. 7. Vertical profile of velocity (u) and (v) at side of the abutment (MS-7.5-5)

5.3. Downstream Flow Field

Figures (8) to (10) show the vertical distribution of the streamwise velocity (u), the lateral velocity (v) and the vertical velocity (w) at different verticals in arbitrary planes (i.e. the planes passing parallel to the flow at the downstream side of the abutment).

The primary vortex and secondary vortex create at the side of the abutment by flow separation extend around the abutment from side in downstream direction to form wake vortices. The wake vortices caused erosion process acting like small tornadoes sucking up material from the bed Figure (1).

The wake vortices are characterized by weak circulation, reversed flow in the opposite direction of the flow in X-direction and upward flow in the Z-direction. Figures (8), (9) and (10) show the vertical distribution of the (u), (v), and (w) velocities. The change of direction (sign) of (u), (v), and (w) velocities indicate the circulation, reversed flow and upward flow occur downstream of the abutment.

The streamwise velocity (u) at the downstream side of the abutment returns to its origin at distance 10 to 12 times abutment protrusion length (L) measured from the abutment centerline.

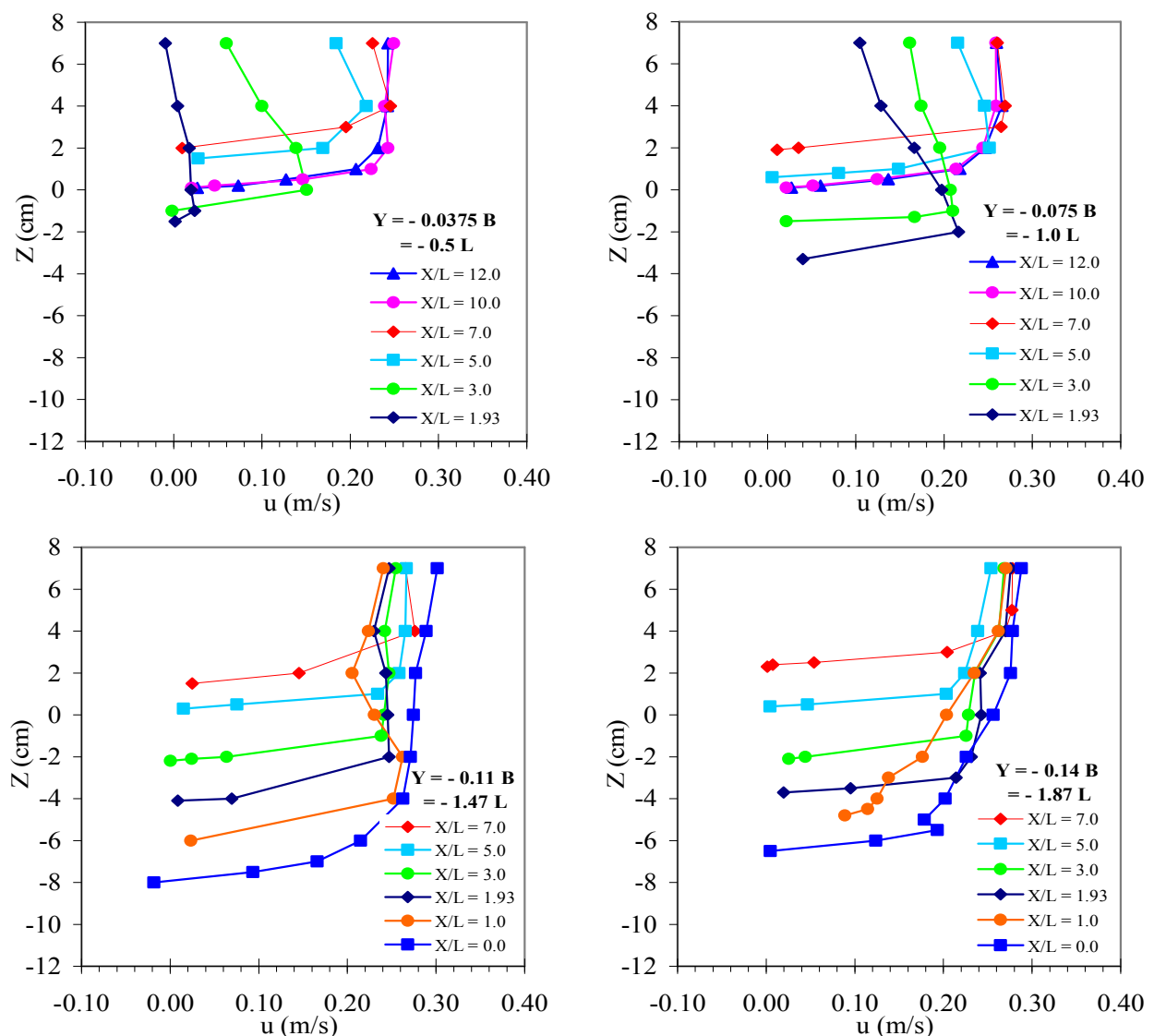


Fig. 8. Vertical profile of velocity (u) at downstream side of the abutment (MS-7.5-5)

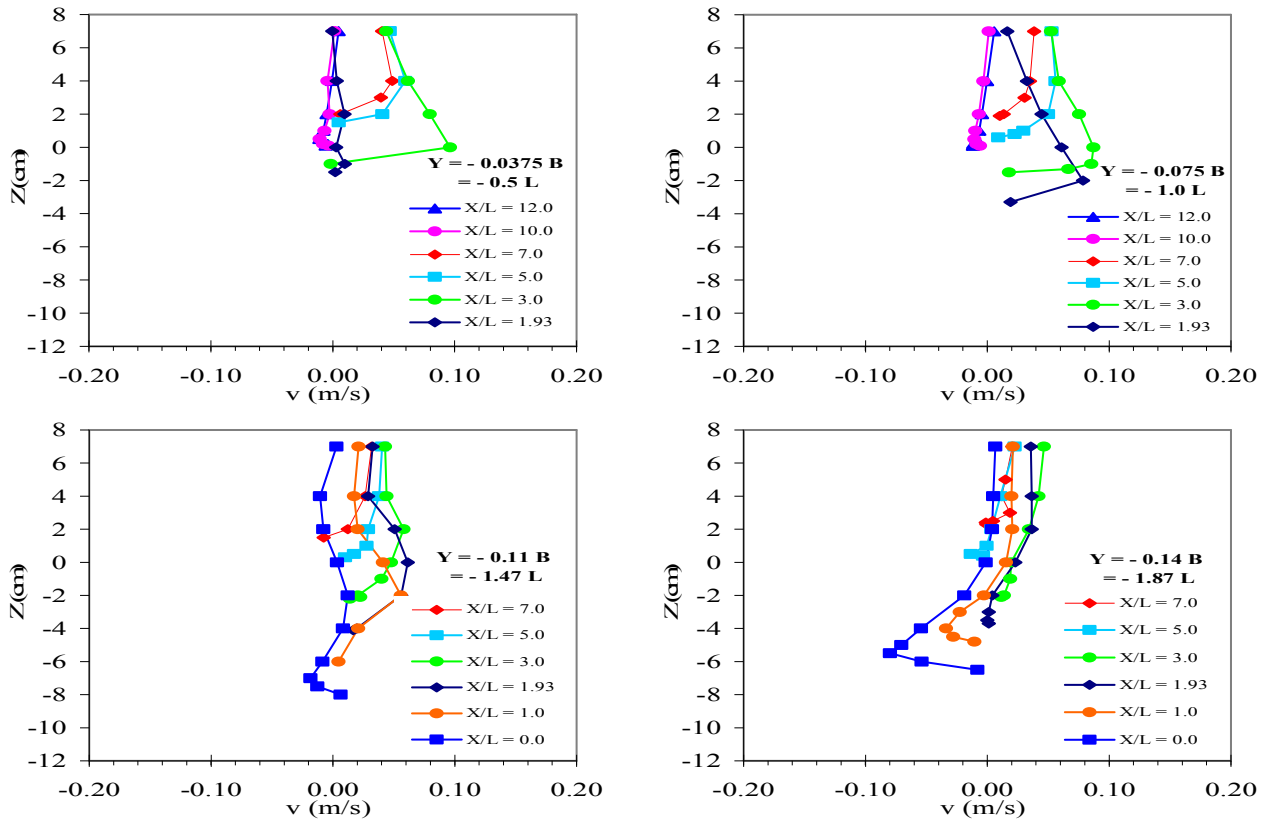


Fig. 9. Vertical profile of velocity (v) at downstream side of the abutment (MS-7.5-5)

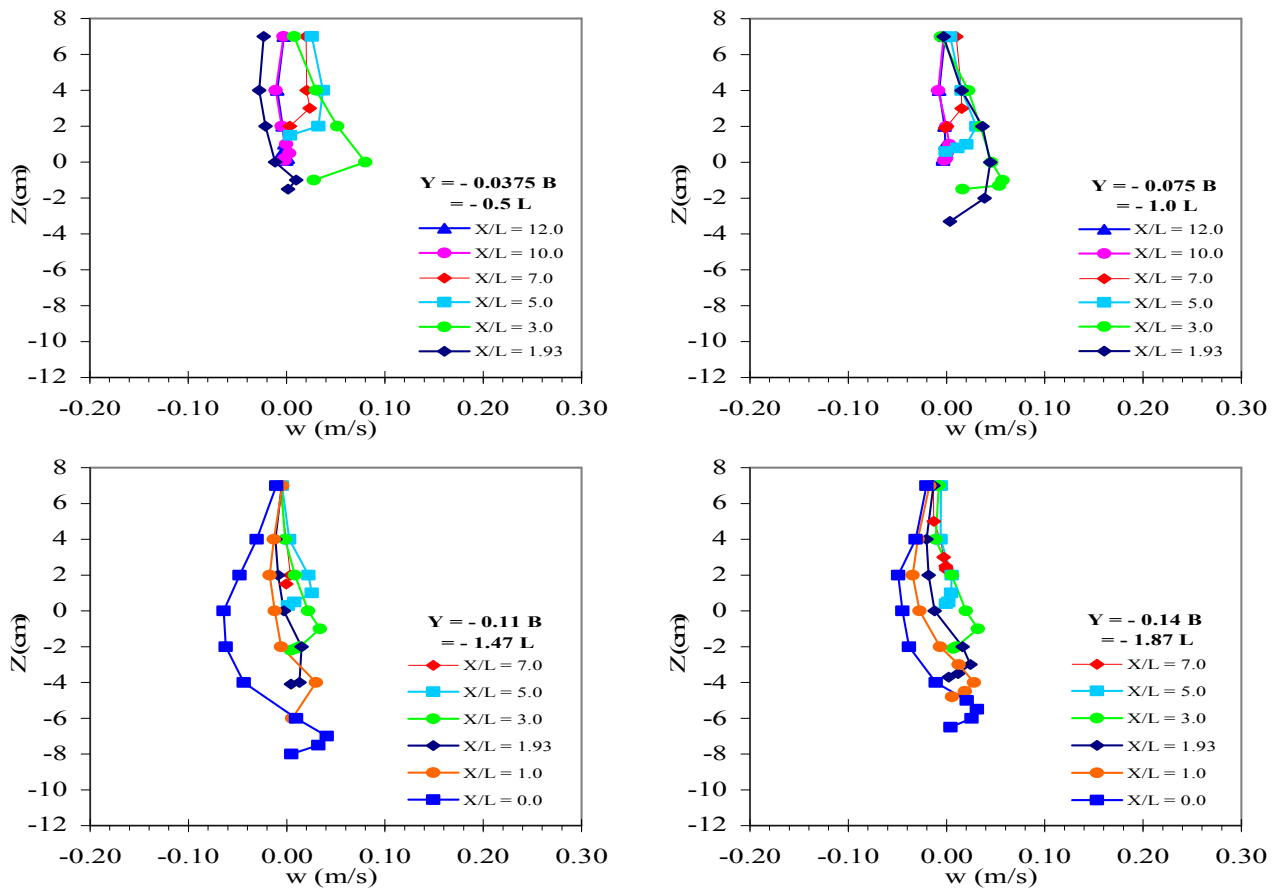


Fig. 10. Vertical profile of velocity (w) at downstream side of the abutment (MS-7.5-5)

6. FLOW FIELD FOR CLAYEY SOIL

The velocity measurements in clayey soil are carried out for the experiment KC-10-11 at equilibrium scour. The experiment has abutment protrusion length = 10 cm, discharge = $0.0619 \text{ m}^3/\text{s}$, flow depth = 0.123 m, approach velocity = 0.50 m/s, and Froude number = 0.46.

6.1. Upstream Flow Field

Figures (11) to (13) show the vertical distribution of the streamwise velocity (u), the lateral velocity (v) and the vertical velocity (w) at different verticals in arbitrary planes (i.e. the planes passing parallel to the flow at the upstream side of the abutment).

In the planes intersecting the abutment, the flow upstream of the abutment starts to decelerate, due to the presence of the abutment, at distance equal 6 times abutment protrusion length (L) measured from the abutment centerline. The deceleration of the flow upstream of the abutment is noticed by a decrease in the streamwise velocity (u) as the flow approached the abutment.

Negative streamwise velocity (u) (reversed velocity) is recorded inside the scour hole Figure (11). This shows that, circulation occurs in the scour hole at the upstream side of the abutment due to the primary vortex Figure (1). The maximum value of reversed velocity (u) is 0.4 times the mean approach velocity.

The stagnation pressure gradient is developed in front of the abutment because the streamwise velocity (u) decreases downward from the surface. The stagnation pressure gradient leads to downward deflection of the flow to form the downward flow at the upstream side of the abutment Figure (1). The downward flow is noticed by negative velocity in the vertical direction (w) at the upstream side of the abutment Figure (13). The strength of downward flow in front of the abutment reaches a maximum just below the bed level when a scour hole was present. The maximum value of downward flow velocity (w) is 0.6 times the mean approach velocity.

Some positive (w) velocity inside the scour hole close to the abutment shows the circulation due to the primary vortex inside the scour hole. The jet created by the downward flow pushes the bed causing it to erode sediment and then rolled up and became part of the primary vortex.

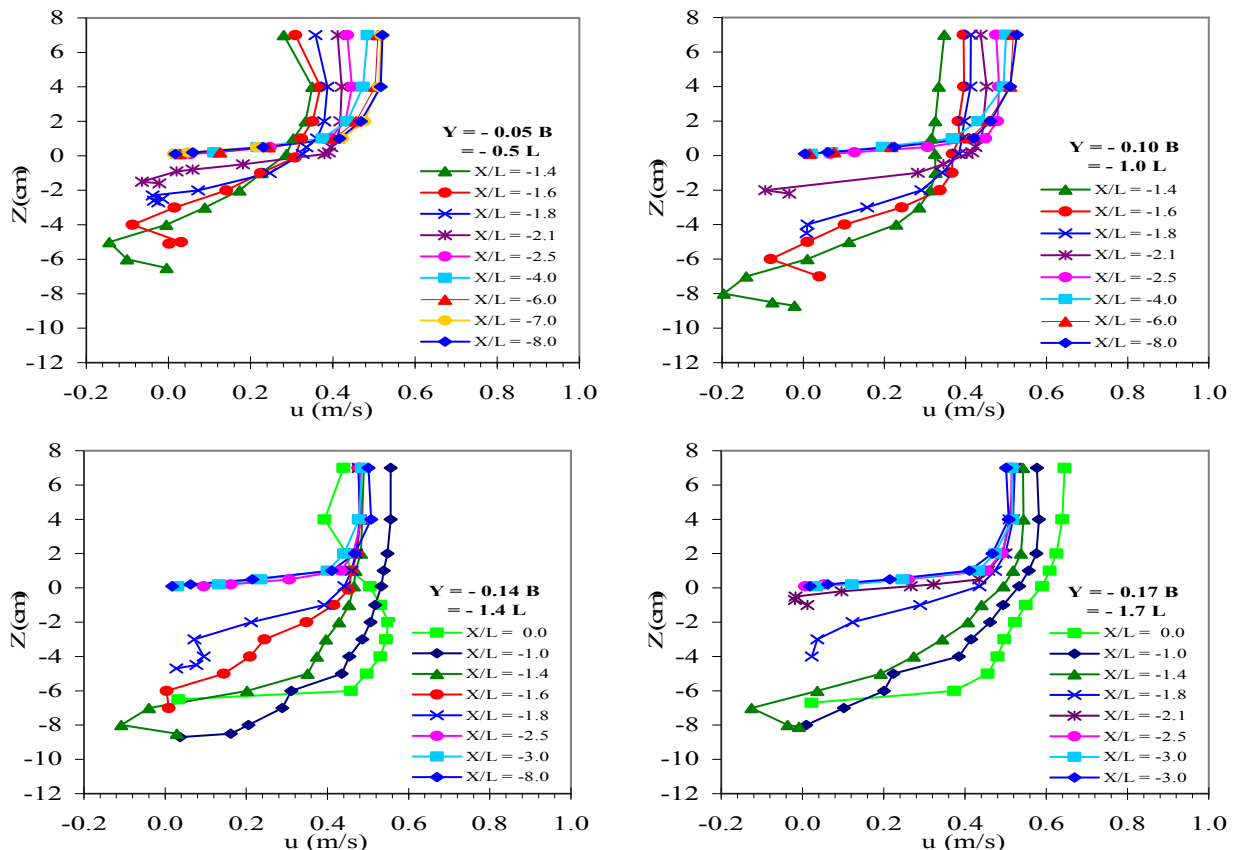


Fig. 11. Vertical profile of velocity (u) at upstream side of the abutment (KC-10-11)

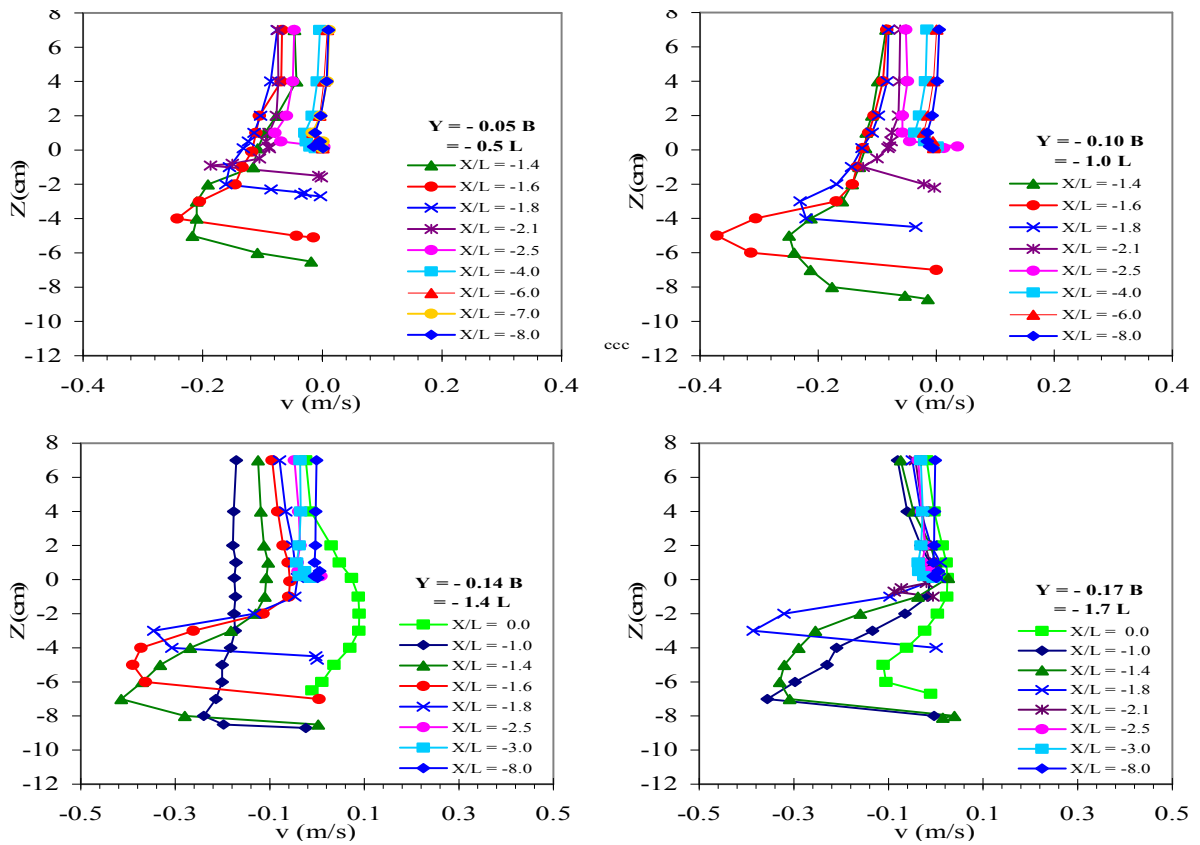


Fig. 12. Vertical profile of velocity (v) at upstream side of the abutment (KC-10-11)

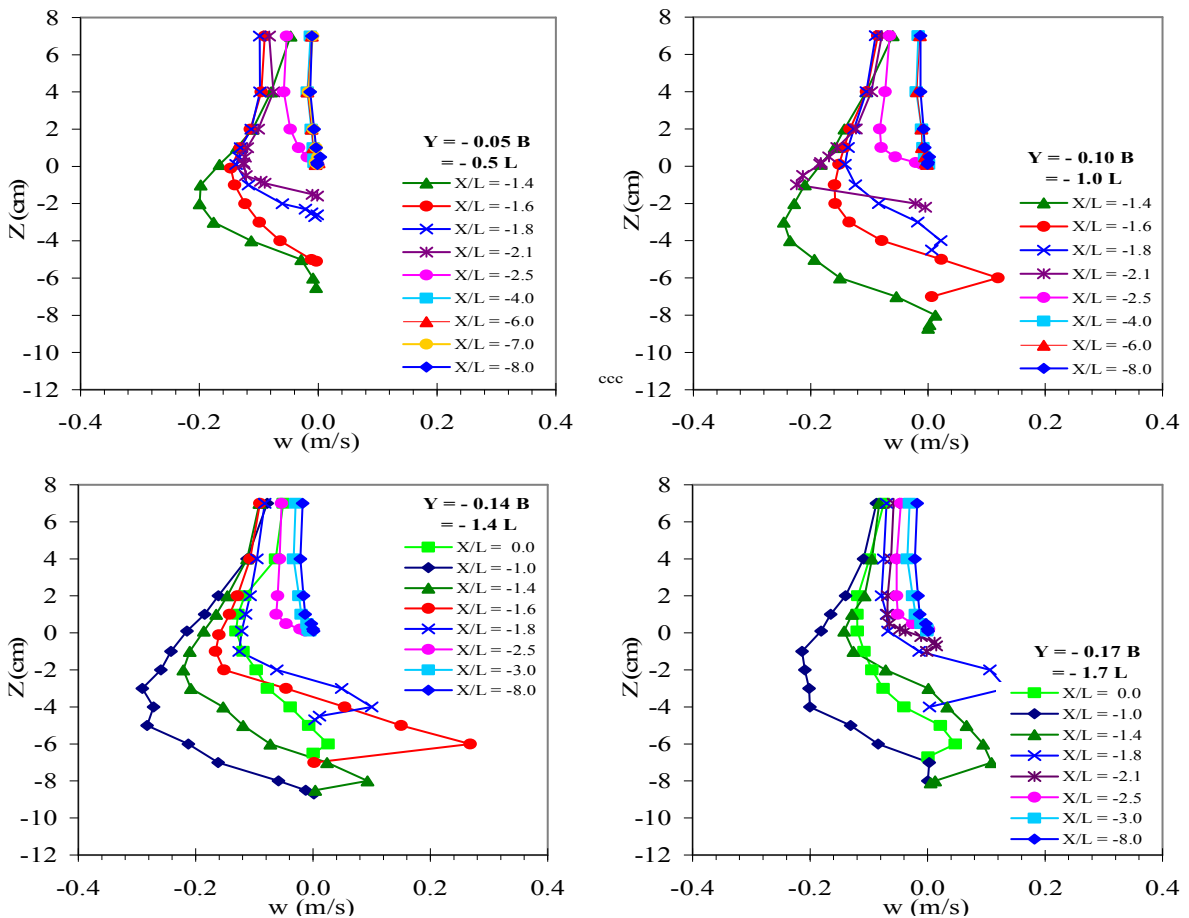


Fig. 13. Vertical profile of velocity (w) at upstream side of the abutment (KC-10-11)

6.2. Flow At The Side Of Abutment

Figure (14) shows the vertical distribution of the streamwise velocity (u) and the lateral velocity (v) at different verticals in planes perpendicular to the flow.

The primary vortex formed at the upstream side of the abutment near the bottom rotates in downstream direction adjacent to the side of the abutment in a spiral motion Figure (1).

The flow separation by the upstream abutment corner creates a surface with a discontinuity in the velocity profile and this leads to the development of secondary vortex. Secondary vortex has an opposite direction of rotation to the primary vortex Figure (1). The circulation due to the primary vortex and secondary vortex at the side of the abutment is indicated by the change of direction (sign) of the local lateral velocity (v) along the vertical distribution of (v) as shown in figure (14).

The streamwise velocity (u) increases adjacent to the side of the abutment due to the flow contraction. The maximum value of streamwise velocity (u) adjacent to the side of the abutment is 1.3 times the mean approach velocity.

Figure (14) shows the vertical distribution of the (u) and (v) velocities at equilibrium scour. Effect of the presence of the abutment on the streamwise velocity (u) and local lateral velocity (v) at the side of the abutment diminishes at distance equal 6 times abutment protrusion length (L) measured from the channel wall in lateral direction.

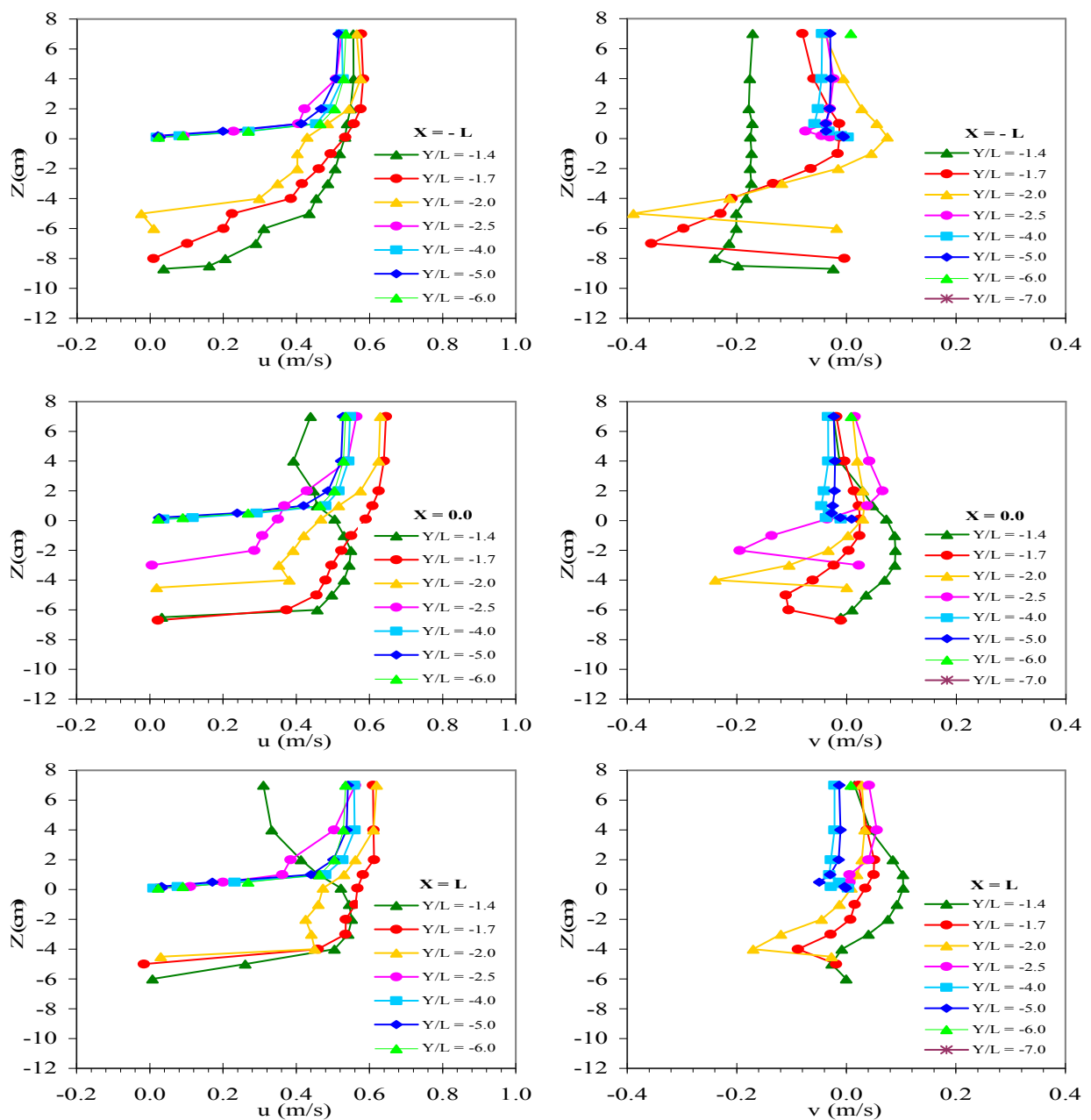


Fig. 14. Vertical profile of velocity (u) and (v) at side of the abutment (KC-10-11)

6.3. Downstream Flow Field

Figures (15) to (17) show the vertical distribution of the streamwise velocity (u), the lateral velocity (v) and the vertical velocity (w) at different verticals in arbitrary planes (i.e. the planes passing parallel to the flow at the downstream side of the abutment).

The primary vortex and secondary vortex creates at the side of the abutment by flow separation extends around the abutment from side in downstream direction to form wake vortices. The wake vortices cause erosion process acting like small tornadoes sucking up material from the bed Figure (1).

The wake vortices are characterized by weak circulation, reversed flow in the opposite direction of the flow in X-direction and upward flow in the Z-direction. Figures (15), (16) and (17) show the vertical distribution of the (u), (v), and (w) velocities. The change of direction (sign) of (u), (v), and (w) velocities indicates the circulation, reversed flow and upward flow occurs downstream of the abutment.

The streamwise velocity (u) at the downstream side of the abutment returns to its origin at distance equal 12 times abutment protrusion length (L) measured from the abutment centerline.

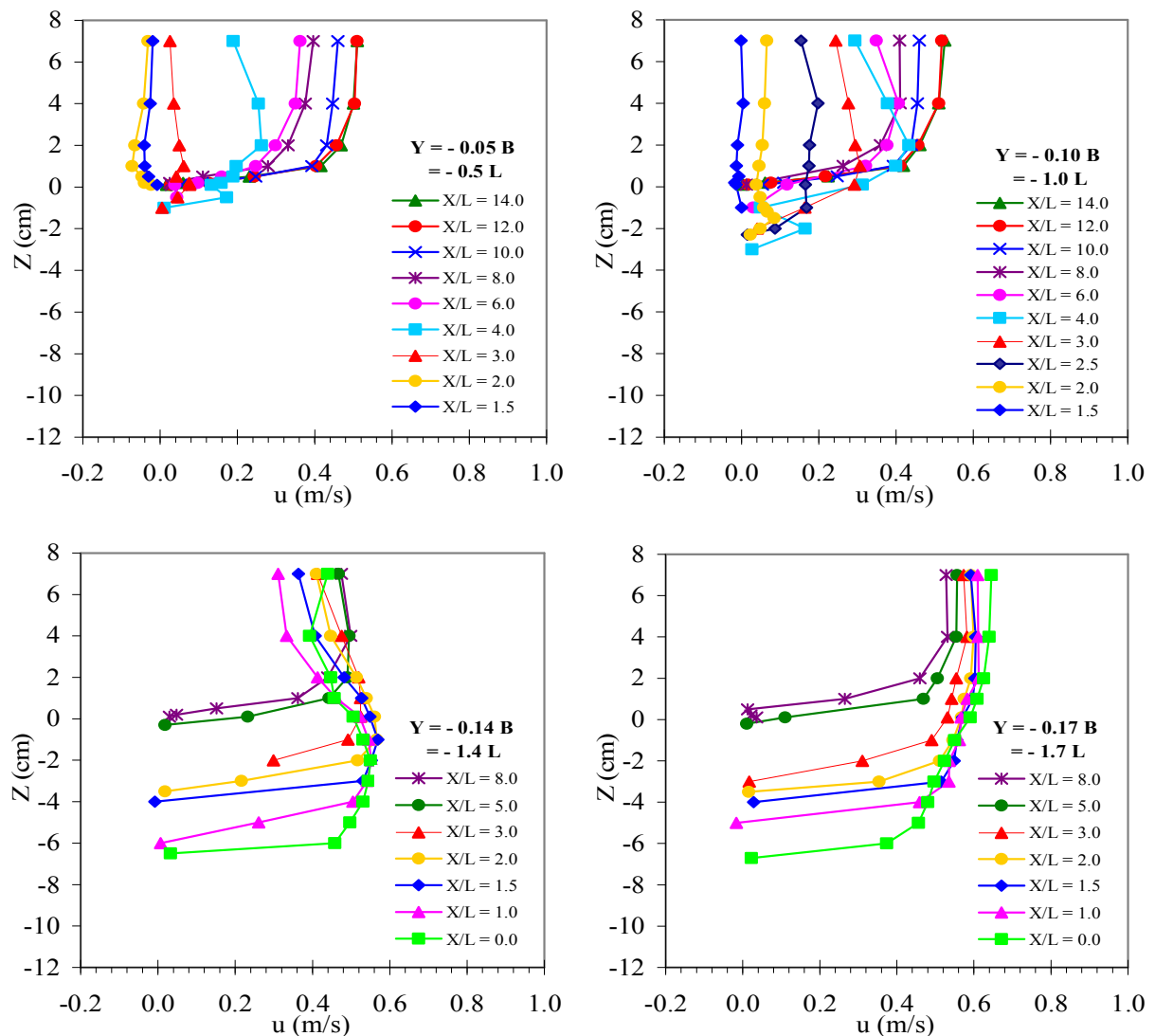


Fig. 15. Vertical profile of velocity (u) at downstream side of the abutment (KC-10-11)

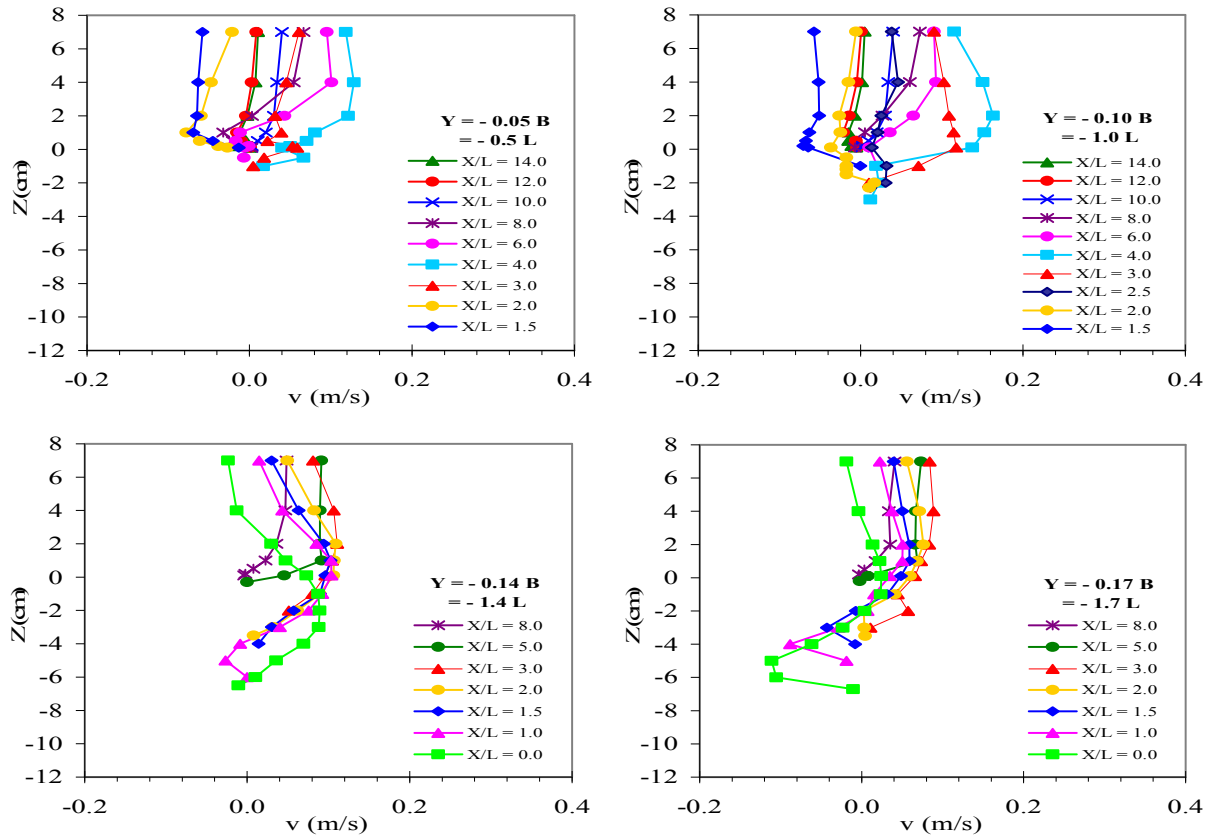


Fig. 16. Vertical profile of velocity (v) at downstream side of the abutment (KC-10-11)

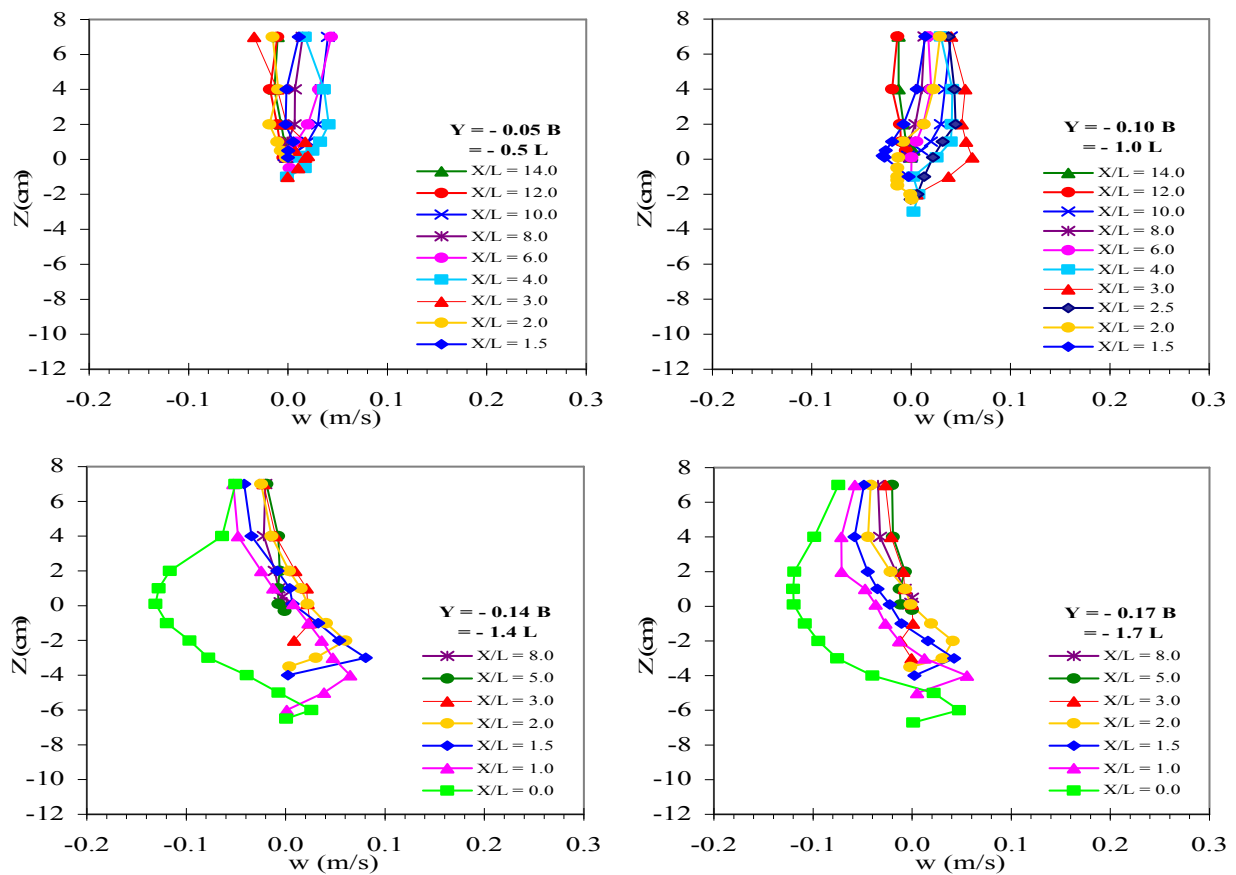


Fig. 17. Vertical profile of velocity (w) at downstream side of the abutment (KC-10-11)

7. COMPARISON BETWEEN FLOW FIELD FOR SANDY AND CLAYEY SOIL

7.1. Upstream Flow Field

The down flow and primary vortex in the scour hole at the upstream side of the abutment are the same for sandy and clayey soil.

7.2. Flow At The Side Of Abutment

The effect of the presence of the abutment on the streamwise velocity (u) and lateral velocity (v) at the side of the abutment is the same for sandy and clayey soil.

7.3. Downstream Flow Field

The wake vortices at the downstream side of the abutment are more pronounced in clayey soil than sandy soil. In sandy soil during the erosion process, once the sediments particles eroded and removed from the bed, they deposit at the downstream side of the abutment.

8. CONCLUSIONS

For flow field around the vertical bridge abutment in both sandy and clayey soil, the following may be concluded:

1. Down flow and primary vortex in the scour hole at the upstream side of the abutment are the same for sandy and clayey soil. Streamwise velocity (u) and lateral velocity (v) at the side of the abutment is the same for sandy and clayey soil. Wake vortex at the downstream side of the abutment is more pronounced in clayey soil than sandy soil.
2. Flow at upstream side of the abutment starts to decelerate at distance 5 to 6 times abutment protrusion length measured from the abutment centerline.
3. Flow at downstream side of the abutment returns to its origin at distance 10 to 12 times abutment protrusion length measured from the abutment centerline.
4. Effect of the presence of the abutment on the streamwise and lateral velocity at the side of the abutment diminishes at distance 5 to 6 times abutment protrusion length measured from the channel wall in lateral direction.

9. NOTATIONS

The following symbols are used in this paper:

- a Abutment length in the flow direction,
- B Flume width,
- C_c Clay content based on weight,
- C_{omp} Compaction degree related to the optimum compaction,
- D_{50} Mean sediment size,
- F_r Upstream Froude number,
- L Abutment protrusion length,
- LI Liquidity index,
- V Upstream approach velocity,
- y Average upstream flow depth,
- u, v, w. Time-averaged velocities in Cartesian coordinates X, Y, and Z respectively.

REFERENCES

1. Ahmed F. and Rajaratnam N., (2000), "Observations on flow around bridge abutment.", *Journal of Hydraulic Engineering ASCE*, Vol. 126, No.1, pp. 51–59.
2. Elzahry E. F. M. (2009), "Scour at bridges abutments in cohesive soil.", Ph.D. Thesis, Department of Civil Engineering, Faculty of Engineering (Shoubra), Benha University, Egypt.
3. Graf W.H. and Istiarto I., (2002), "Flow pattern in the scour hole around cylinder.", *Journal of Hydraulic Research, IAHR*, Vol. 40, No. 1, pp. 13-20.
4. Kwan T.F., (1988), "Study of abutment scour.", Rep. No. 451, School of Engrg., The Univ. of Auckland, New Zealand.
5. Kwan T.F. and Melville B. W., (1994), "Local scour and flow measurements at bridge abutments.", *Journal of Hydraulic Research, IAHR*, Vol. 32, No. 5, pp. 661-673.
6. Lim S-Y., (1997), "Equilibrium Clear Water Scour Around an Abutment.", *Journal of Hydraulic Engineering, ASCE*, Vol. 123, No. 3, pp. 237-243.
7. Mostafa T. M. S., (2003), "Experimental modeling of local scour in cohesive soils.", PhD dissertation, University of South Carolina, Columbia, SC.
8. Nortek (2000), "ADV Users Manual.", Nortek A S, Norway.
9. Raudkivi A. J., (1990), "Loose Boundary Hydraulics.", 3rd edition, Pergamon Press, New York, USA.
10. Raudkivi A.J., (1986), "Functional Trends of Scour at Bridge Piers.", *Journal of Hydraulic Engineering, ASCE*, Vol. 112, No. 1, pp. 1-13.